Journal of Molecular Liquids 328 (2021) 115406

Contents lists available at ScienceDirect

Journal of Molecular Liquids

journal homepage: www.elsevier.com/locate/molliq

COSMO-SAC-supported evaluation of natural deep eutectic solvents for the extraction of tea polyphenols and process optimization

Zhifang Cui, Alexandra Victoria Enjome Djocki, Jinhao Yao, Qianwen Wu, Dequan Zhang, Shiwei Nan, Jun Gao, Chunlu Li *

College of Chemical and Biological Engineering, Shandong University of Science and Technology, Qingdao 266590, China

ARTICLE INFO

Article history:
Received 27 September 2020
Received in revised form 10 January 2021
Accepted 13 January 2021
Available online 20 January 2021

Keywords:
Natural deep eutectic solvents (NADESs)
Tea polyphenols (TPs)
Epigallocatechin gallate (EGCG)
Response surface methodology (RSM)
Extraction
COSMO-SAC (conductor-like screening model for segment activity coefficient)

ABSTRACT

To reduce the environmental pollution caused by organic solvents and improve the extraction efficiency, a range of natural deep eutectic solvents (NADESs) was explored for the extraction of green tea polyphenols (TPs). The use of the NADESs, especially ChCl/EG (Choline chloride/Ethylene glycol, molar ratio 1:2), can increase extraction efficiency when comparing with the traditional solvents. Then response surface methodology (RSM) was used for the optimization of TPs extraction with ChCl/EG. The perfect regression prediction model was generated and the highest TPs extraction yield of 20.12% was achieved, highlighting the potential of NADES for TPs extraction.

Meanwhile, the applicability of COSMO-SAC (Conductor-like screening model for segment activity coefficient) for evaluation of TPs extractability in different solvents was investigated. Epigallocatechin gallate (EGCG) was employed as the TPs model solute. Geometry optimization and energy optimization of EGCG and these solvents were performed via COSMO-SAC. The extraction performance of the solvents was interpreted by the analysis of activity coefficient at infinite dilution ($\gamma\infty$). The result showed that the higher the extraction yield, the lower the $\ln\gamma\infty$. The σ-profile and the interaction energy (E_{INT}) were generated to analyse the molecular interaction between solvent and solute. It was demonstrated that the combination of a strong hydrogen bond acceptor (HBA) - ChCl, with a relatively weaker hydrogen bond donor (HBD) - EG, resulted in a NADES (ChCl/EG) with a stronger affinity to TPs. This work provided both experimental and intermolecular insight to help choose effective solvent for bioactive components extraction in further research.

1. Introduction

Tea polyphenols (TPs) are the main bioactive constituents of green tea with a wide variety of beneficial health effects, such as blood-pressure and blood-lipid lowering, anti-oxidation, anti-inflammation, anti-bacteria and anti-aging. Green tea polyphenols make up 16–30% of the dry weight of fresh leaves [1], and the majority of which are catechins [2]. Among the four main catechins found in TPs [3], epigallocatechin gallate (EGCG) possesses the strongest antioxidant activity [4,5], and it accounts for 55–70% of the total TPs [6,7]. Due to the potential benefits of the TPs, many studies have been conducted to maximize the extraction yield of TPs from green tea [8]. The extraction efficiency of a specific natural product from the plant is usually dependent on the choice of solvent and method of extraction. Although water is the cheapest and safest medium [9], it demonstrates relatively low TPs extraction yield comparing with organic solvents. Different conventional organic solvents have been widely studied for TPs extraction so far [10]. However, organic solvents are usually flammable, explosive and can pollute the environment, sometimes even leave unacceptable residues in extracts, which limits the usage of TPs. In recent years, many novel methods were reported for the extraction of bioactive compounds, such as ultrasound-assisted extraction [11], microwave-assisted extraction [12] and advanced enzyme-assisted extraction [13]. Nevertheless, costly equipment and complex operation were employed in these studies. In that view, the additional research that can promote TPs extraction using an environment-friendly solvent with low cost and simple operation is needed [14].

As a new generation of ionic liquids (ILs), deep eutectic solvents (DESs) have attracted much attention recently, and have been widely used to extract active compounds from plants [15]. They are typically prepared by simply mixing a hydrogen bond acceptor (HBA) with a hydrogen bond donor (HBD) [16]. The polarity of DESs can be fine-tuned by simply changing the combination of HBA and HBD, thus allowing for tailor-made selectivity for extractions and separations of various solutes [17]. Natural deep eutectic solvents (NADESs) are composed of two or more bio-derived compounds, i.e., organic acids, sugars, alcohols, amines. The non-toxicity, biodegradability and sustainability of NADESs

* Corresponding author.
E-mail address: enmaster@sdust.edu.cn (C. Li).

https://doi.org/10.1016/j.molliq.2021.115406
0167-7322/

distinguish them from other categories of DESs. NADESs have recently been widely used as an extraction medium for rutin [18,19], flavonoids [20–22] and phenolic compounds [23,24] with various plants as raw material. Despite the extensive research on NADESs application as an extractant, most of them mainly focus on the optimization of extraction parameters through experiment. To the best of our knowledge, few of these literatures explored the interaction between solvent and solute from a quantum chemical way.

Recently, a thermal dynamic modelling based on quantum chemical calculations-COSMO (Conductor-like screening model) was utilized as a tool for modelling and predicting of liquid-liquid equilibrium [25–27], among which COSMO-SAC (for segment activity coefficient) and COSMO-RS (for real solvent) are the two most commonly used models. Several previous investigations have demonstrated that COSMO has the acceptable quantitative ability of solvent extraction equilibrium prediction in DES-involved systems [28,29]. However, it should be noted that most of the reports involving COSMO mainly focused on the liquid-liquid separation. Zurob and his co-workers [13] concluded that COSMO could be used to predict the behaviour of DESs for extraction of hydroxytyrosol from olive leaves, which was the one, as far as we know, exploring the application of COSMO in solid-liquid extraction.

Based on the previous awareness, the specific objectives of this study were to (1) investigate the performance of TPs extraction from green tea using different choline chloride (ChCl)-based NADESs, (2) choosing EGCG as TPs model solute, use COSMO-SAC for quantum chemical simulation, to calculate the σ-profile and the interaction energy (E_{INT}), thus understand the molecular interaction between solute and different solvents, (3) correlate thermodynamic activity coefficient at infinite dilution of EGCG in the solvent with experimental values of TPs extraction efficiency, to check the applicability of COSMO-SAC in extractant prescreening of TPs extraction, (4) with the screened optimal NADES, systematically optimize the extraction process using response surface methodology (RSM) with BOX-Behnken Design (BBD). Aside from this practical goal, the present work highlights the potential application of theoretical and experimental correlation to evaluate the efficient solvents that could be applicable for the extraction of bioactive compounds.

2. Material and methods

2.1. Materials

Low rank green tea was purchased from the local market of Qingdao, Shandong, with the brand of LaoShan Green Tea. It was dried overnight in an oven at 80 °C to constant weight, ground into fine powder and sieved (100 mesh). The powder was stored -8 °C in an air-tight and light resistant container until use. Choline chloride (>98%), Ethylene glycol (>98%) were purchased from Shanghai Macklin Biochemical Co., Ltd. Tea polyphenol (High purity grade, ≥98%) was manufactured by BioDuly Biochemical Reagent Co., Ltd., Nanjing, China. All the other chemicals were analytically pure and purchased from Tianjin Kermel Chemical Reagent Co., Ltd. (Tianjin, China). UV–Vis Spectrophotometer (T6 New century, Pgeneral, Beijing, China). High speed refrigerated centrifuge (TGL-16M, Xiangyi, Changsha, China).

2.2. NADESs preparation

Choline chloride (ChCl) was used as the HBA of NADESs in our study. Five HBDs were investigated, including two alcohols, ethylene glycol and glycerol, one sugar, glucose, two organic acids, oxalic acid and citric acid. The components of the five NADESs (including the molar ratio of HBA to HBD) investigated in the paper are listed as in Table 1. Certain amounts of HBA and HBD with the according molar ratio were weighed and then added into a 500 mL round bottom flask, magnetically stirred at 80 °C, until the mixture was uniform and transparent. Then the homogenous NADES was cooled down to room temperature and transferred into an airtight container and stored in a desiccator until use.

Table 1
DESs composition.

DESs Abbreviation (HBA/HBD)	HBD	Molar ratio (HBA: HBD)
ChCl/EG	Ethylene Glycol	1:2
ChCl/Gly	Glycerol	1:2
ChCl/Glu	Glucose	1:1
ChCl/OA	Oxalic Acid	1:1
ChCl/CA	Citric Acid	1:1

2.3. Solvent screening for TPs extraction

Five NADESs as in Table 1 were investigated as solvents for TPs extraction. For comparison, two traditional solvents, water and ethanol were also studied in our work. 0.25 g tea powder and 10 g of solvent (liquid to solid ratio of 40) were mixed well in a 20 mL crimp vial. The vial was sealed and put into a magnetic stirring water bath at 70 °C for 3 h. Duplication was done for the extraction of TPs with each solvent. The extracts were centrifuged at 4, 000*g* for 25 min. The clarified supernatant was collected for TPs measurement.

2.4. TPs quantitative analysis

The content of TPs was determined using the modified ferrous tartrate colorimetry method [30]. During measurement, 1 mL standard solution which contained 50–400 μg tea polyphenol was mixed with ferrous tartrate and 3 mL phosphorous buffer (1/15 mol/L, pH 7.5). After mixing well with the help of a vortexer, absorbance at 540 nm was measured by a UV–Vis spectrophotometer and the standard curve was drawn. When doing the sample assay, 1 mL diluted sample (clarified supernatant extracts) was added instead. TPs concentration (c) was obtained according to the corresponding standard curve. During analysis, distilled water and the according solvents were used as blanks for standard and the extracted sample, respectively. Each sample was measured in triplicate.

The extraction yield was defined as the following equation.

$$\text{Extraction Yield } (\%) = \frac{c \times D \times V}{m_0} \times 100$$

where c (mg/mL) is the TPs concentration of the diluted sample, D is the dilution factor, V (mL) is the total volume of the clarified extracts. m_0 (mg) is the tea powder used for extraction.

2.5. Molecular optimization and COSMO-SAC analysis

The Dmol3 module in the Material Studio 7.0 (Accelrys, U.S.A.) was adopted for the computation. During the simulation, EGCG was used as a TPs model solute. EGCG and each solvent were undergone geometry & energy optimization. As NADES consists of HBD and HBA, geometry & energy optimization of HBD and HBA was carried out before dealing with them as one compound. Then they were treated as one molecule and underwent structure & energy optimization to obtain the NADES's σ-profile [31]. Moreover, the interaction energy between solvent and EGCG was calculated [32]. The settings were described in detail in the previous work [33]. Meanwhile, the σ-profile analysis was done by using the COSMO-SAC model [34,35]. After the final optimization, the COSMO information of those molecules was generated. Then, the polarity information for each component was obtained. The detailed explanation of the open source COSMO-SAC model and its calculations were introduced in our previous study and were not discussed here [36]. Besides, the activity coefficient at infinite dilution ($\gamma\infty$) of

EGCG in different solvents was also obtained, which can be used to correlate the extraction capacity of solvents on a thermodynamics basis.

2.6. Optimization of the TPs extraction

RSM is a valuable mathematical methodology for optimization of responses. The influence of different variables as well as the interaction effects of these variables on the process response can be evaluated [37]. Tea powder (0.20 g) was added into a 20 mL crimp vial and mixed well with certain grams of the screened NADES. The vial was sealed and put into a stirring water bath for TPs extraction. Based on the results of the primary single factor experiments, three levels of four variables, i.e., extraction time, temperature, liquid to solid ratio and water content were determined. Water content was investigated to increase the mass transfer rate during extraction and thus save the extraction time. RSM with Box-Behnken Design (BBD) was used for the optimization of the extraction. The Design-Expert 8.06 was employed in the regression and graphical analyses of data. The statistical analysis of the model was performed to evaluate the analysis of variance (ANOVA). Levels of the variables are listed in Table 2.

The experimental design consists of 29 runs, including five replicates of the central point to estimate the pure error.

3. Results and discussions

3.1. Solvent screening for TPs extraction

Extraction of TPs with different solvents, including five NADESs and two traditional solvents, water and ethanol, was carried out. The extraction yield is shown in Fig. 1. It can be observed that three NADESs presented competitive extraction values with ethanol, among which ChCl/EG had the best performance, while the extraction yield of TPs with water was the lowest.

Polarity or hydrophobicity is one of the most important factors to consider when designing a suitable extraction solvent for a specific product. One of the most widely used descriptors of molecule's lipophilicity/hydrophobicity is log*P*, which is the logarithm of the partition coefficient between octanol and water. Usually, the higher the log*P*, the higher the lipophilicity (hydrophobicity), while the lower the polarity [38]. There was no direct experimental data about the log*P*s of all TPs components. It was reported that the log*P* of epicatechin (the one with the simplest molecular structure among the four compounds of catechin) was about 0.4 [39]. Since other TPs are epicatechin derivates by esterification, it could be inferred that in general, TPs should have log*P* higher than 0.4, and be a group of medium ($0.028 \le \log P \le 1.31$) or even high ($\log P > 1.31$) hydrophobic compounds. For example, the log*P* of EGCG was about 1.2 [39]. Ethanol has a log*P* of about −0.12 [39], which belongs to the range of low hydrophobicity. Although the data about the properties of NADESs was scarce, NADESs formed with organic acid was more polar than those derived from alcohol or sugar [13]. Therefore, in our case, for extraction of TPs which was medium or high hydrophobic, NADESs with lower polarity, such as ChCl/EG, ChCl/Gly and ChCl/Glu could achieve relatively high extraction yield, compared with the polar solvents, for example, ChCl/CA, ChCl/OA and water. These extraction results can be explained with the principle of "like dissolves like".

Table 2
Variables and levels of the BBD.

Level	Variable			
	A	B	C	D
	Time (min)	Temperature (°C)	Liquid to solid ratio	Water content (%)
−1	20	70	20	20
0	40	82.5	40	30
1	60	95	60	40

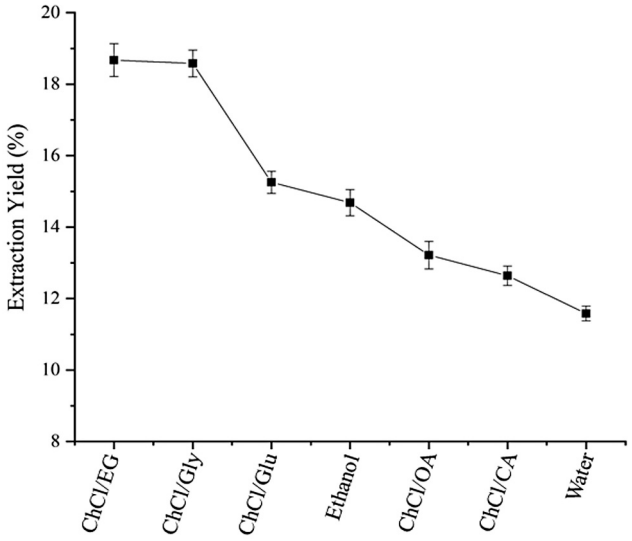

Fig. 1. TPs extraction yield with different solvents.

Among all the solvents investigated, ChCl/EG can be highlighted, which demonstrated the highest extraction yield of about 18.68%. In our study, ChCl was used as HBA of all the NADESs. It was obvious that by simply changing HBD from EG to CA, the TPs extraction yield decreased greatly to about 12.64%, which implied that the proper design of NADES is very important during extraction. On the other hand, compared with the traditional solvents, the fine tunability of NADES enables its wide application prospects as an extraction solvent [19], while few works of literatures went behind the experiment and tried to explain the so-called "optimal" solvent from a theoretical way [40].

As far as we know, the general rule "like dissolves like" is an ancient chemical recipe, which is relatively ambiguous under certain circumstances [41]. Although log*P* value being useful to give a rough estimation about the solubility of a chemical in the solvent, it is not able to give conclusive insights into the properties of solvent and solute [42]. Further information is needed to better understand the molecular interactions between NADESs and the target products for solvent screening.

Through COSMO-based thermodynamics calculation, Klamt and his coworkers evaluated the surface charge densities (σ-surface) and σ-profiles of different solvents and tried to explain why some molecules liked each other, while others did not [43]. In this case, to provide a better understanding of the mutual solubilities during extraction, COSMO-SAC analysis was carried out for the molecular simulation of the solvent and solute in our work.

3.2. Theoretical support of TPs extraction with COSMO analysis

The chemical structure, surface charge density (σ-surface) and σ-profile of EGCG are presented in Fig. 2, to evaluate the solute based on quantum chemical calculations.

The 3-D σ-surface of EGCG revealed the non-polar and the polar regions of the molecule. The polar region is due to the polarization of -OH group since the difference of electronegativity existing between H (blue) and O (red) atoms. The non-polar region, is the characteristics of the neutrally charged zones, corresponding to the C (green) and H (blue) atoms in three benzene rings [44] and one pyranoid ring of the molecule.

The σ-profile obtained is one of the most important molecule-specific properties, which is the distribution of the screening surface density of the molecule. The σ-profile is usually divided into three

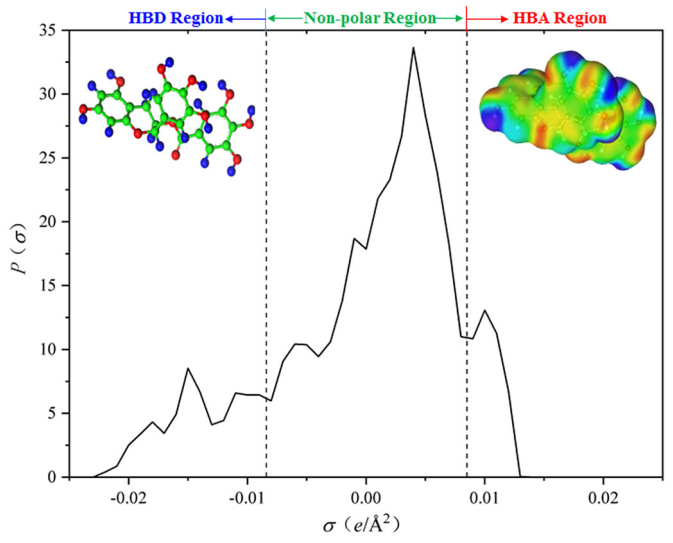

Fig. 2. The chemical structure (upper left), surface charge density (σ-surface, upper right) and σ-profile of EGCG.

regions [45]: the HBD region ($\sigma < -0.0084$ e/Å^2), the nonpolar region (-0.0084 e/Å$^2 < \sigma < 0.0084$ e/Å^2), and the HBA region ($\sigma > 0.0084$ e/Å^2). These three regions are separated by the threshold value for hydrogen bonding $\sigma_{hb} = \pm 0.0084$ e/Å^2 as illustrated in Fig. 2. Generally speaking, a σ-profile in the region of $\sigma < -0.0084$ e/Å^2 and $\sigma > 0.0084$ e/Å^2 indicates its hydrogen-bond donor ability and its hydrogen-bond acceptor ability, respectively. It was concluded by Klamt that σ-regions beyond ± 0.01 e/Å^2 was strongly polar and could be act as a potential HBD ($\sigma < -0.01$ e/Å^2) or HBA ($\sigma > 0.01$ e/Å^2). The endpoints of the σ-profiles were frequently used when comparing polarity of different molecules [43,46].

As shown in Fig. 2, the σ-profile of EGCG was mainly distributed within the range of -0.022 e/Å$^2 < \sigma < 0.013$ e/Å^2. The height of peaks in σ-profile stands for the statistical numbers of the surface segments of the molecule possessing the similar polarity. The peaks at the nonpolar region (-0.0084 e/Å$^2 < \sigma < 0.0084$ e/Å^2) seemed quite high, which means that EGCG molecule has large quantities of nonpolar segments on its σ surface. This is in agreement with its property of moderate hydrophobicity (log$P = 1.2$ from the above discussion). During the discussion of the σ-profile, the range outside ± 0.0084 e/Å was usually the keynote due to the fact that hydrogen bond interaction energy was about an order of magnitude higher than that of Van der Waals-Bond, while the later was mainly responsible for the interaction in non-polar range [47]. When evaluating polar regions in Fig. 2 ($\sigma < -0.0084$ e/Å^2 or > 0.0084 e/Å^2), note that owing to the sign inversion, the σ-profile demonstrated that the peaks located at the negative polar coordinate (left side) are due to the positively polar H atoms in -OH group, while the peaks positioned at the positive polar coordinate (right side) are assigned to O atoms in -OH and an ester group. These polar regions of EGCG caused by polar surface segments can interact with other opposite polar surface segments in solvents. It was demonstrated that the extension of its σ-profile into the strongly polar regions, i.e., -0.022 e/Å$^2 < \sigma < -0.01$ e/Å^2 (left) and 0.01 e/Å$^2 < \sigma < -0.013$ e/Å^2 (right) was asymmetric, which implied EGCG had more positive polarity surface area [48]. It was supposed to be in a electrostatic misfit due to the fact that hydrogen could not find appropriate counterparts [43]. Hence, EGCG was more inclined to be a HBD, and thus would show more affinity toward those showing HBA potential in the solution.

3.2.1. Correlation between COSMO-SAC prediction and experimental result

The molecular optimization of solvents was also simulated using COSMO-SAC. The σ-profiles of EGCG, five NADESs, as well as those of two traditional solvents, water and ethanol, were also calculated. The activity coefficients at infinite dilution ($\gamma\infty$) of EGCG in different solvents were achieved which can be used for the evaluation of the extracting capacity of those solvents. Then ln$\gamma\infty$ was calculated and plotted as shown in Fig. 3. In our study, the one possessed the lower ln$\gamma\infty$ (ChCl/EG) demonstrated the higher TPs extraction yield, and vice versa.

There are several reports about the application of COSMO-based modelling for prediction of the extraction performance with ILs or NADES. Zurob et al. [13] studied the design of NADES for hydroxytyrosol extraction from olive leaves. The simulated $\gamma\infty$ value showed an opposite trend with the experimentally extracted hydroxytyrosol concentration, which was consistent with our result. Through the COSMO model, Wlazlo et al. [49] evaluated the accuracy using $\gamma\infty$ for the prediction of the partition of various organic solutes from different groups in 12 ILs. The results showed that it was difficult to make an unambiguous conclusion. The model can offer both qualitative and quantitative predictions in some cases (i.e., polar compounds), but not in all cases, i.e., aromatic hydrocarbons and ethers. Therefore, the experiment was recommended to be done to validate the simulated data. For the investigated model solute EGCG and different solvents in our work, the extraction of TPs with those solvents could be qualitatively predicted with the help of COSMO-SAC.

3.2.2. σ-profile for molecular interaction analysis between EGCG and solvents

Due to the charge-related and molecule-specific characteristics, the σ-profile of the solvent was usually evaluated when trying to screen the suitable solvent for the extraction of a solute [50]. The extraction performance of the solvent was interpreted from the view of molecular interaction with the help of their σ-profiles.

In our study, a naturally derived and most commonly studied HBA, ChCl was investigated. Its σ-profile is illustrated in Fig. 4. It can be seen that O atom (from OH- group) and Cl^- anion of ChCl, corresponded to two broad and high peaks in the region 0.0084 e/Å$^2 < \sigma < 0.02$ e/Å^2, which implied its potential to be a good HBA in the solution [51]. The negative σ value of about -0.016 e/Å^2 was attributed to the H atom from OH- group. The peak at about -0.008 e/Å^2 represented positive charges of the N atom, while peaks at non-polar regions were due to the methyl and ethyl groups of ChCl [52]. Meanwhile, for the evaluation of the possible molecular interaction between HBA and HBD, all the σ-profiles of the HBDs were also computed.

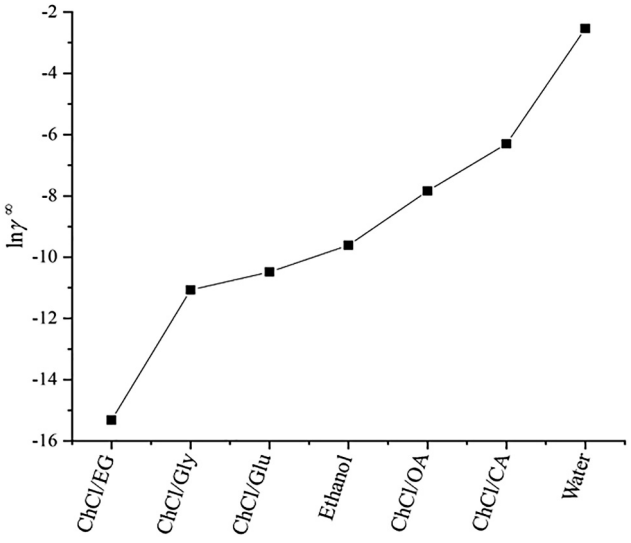

Fig. 3. The logarithmic diagram of activity coefficient at infinite dilution of EGCG in different solvents.

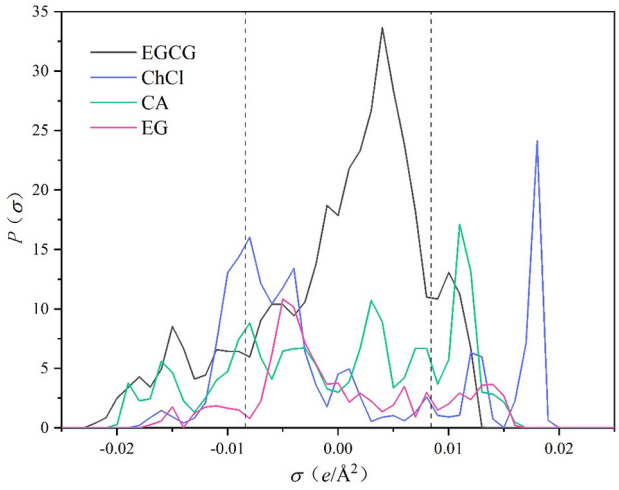

Fig. 4. σ-profiles of EGCG, ChCl and typical HBDs (CA and EG).

For the sake of simple and brief illustration, Fig. 4 only shows two typical HBDs for demonstration, i.e., ethylene glycol (EG) and citric acid (CA). Since the acidic hydrogen was much more polar than those of hydroxyl groups in EG [43], CA had a longer distance away from the negative threshold (<-0.0084 $e/Å^2$). On the other hand, their endpoints at the positive side (HBA region) were almost overlapping, which implied that CA seemed to be a stronger HBD than EG.

For further comparison of the interaction of EGCG with different solvents, the σ-profiles of the solute, two traditional solvents, water and ethanol, two typical NADESs, ChCl/CA and ChCl/EG, in this case, are shown in Fig. 5.

As observed, compared with σ-profiles of ChCl, CA and EG from Fig. 4, the interaction between hydrogen of HBD and Cl^- anion of ChCl resulted in modest decrease of the endpoints at both sides of the σ-profiles (negative & positive), as shown in Fig. 5 (ChCl/CA and ChCl/EG). Meanwhile, heights of the peaks at polar regions decreased to some extent. All these were reasons causing lower melting point of the eutectic mixture [53,54]. During the formation of the DES, contribution from non-polar region was evaluated sometimes but normally not determinant, owing to the fact that the interaction strength from Van der Waals-Bond was very weak [55]. From Fig. 5, it was illustrated that the entire σ-profile of ChCl/CA was in the range of -0.02 e/Å^2 $< \sigma <$ 0.0182 e/Å^2, while that of ChCl/EG was about -0.0168 e/Å^2 $< \sigma <$ 0.0191 e/Å^2 [56]. It was demonstrated that when treated as an

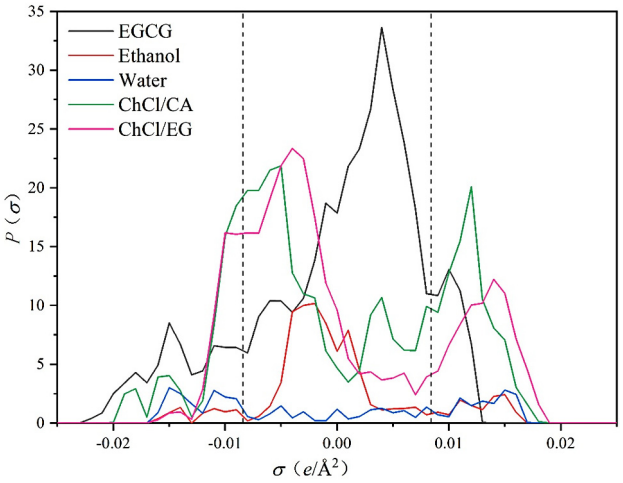

Fig. 5. σ-profiles of EGCG (epigallocatechin gallate) and different solvents.

integral component, a combination of stronger HBD, CA, with ChCl (HBA), formed a NADES (ChCl/CA) which showed stronger HBD ability when comparing with ChCl/EG.

One the other hand, based on the discussion about the σ-profile in Fig. 2, EGCG is inclined to be a HBD in the solution, thus it competed with the HBD of the solvent when doing the extraction. If the NADES itself had strong HBD potential, the EGCG would be in a competitive disadvantage status during extraction.

When comparing the TPs extraction yield from experiment, the combination of ChCl (HBA) with stronger HBD potential, CA in this case, resulted in a NADES of ChCl/CA with a low extraction yield for the solute TPs, which is shown in Fig. 1.

Gonfa and his coworker [57] studied the screening of suitable solvent for natural gas dehydration, they concluded that cation with strong hydrogen bond acidity combining with anion with strong hydrogen bond basicity resulted in an IL with low affinity for the solute. Thus, it could be inferred that the strong hydrogen bond interaction between ChCl and CA led to the lower affinity of the NADES for the TPs, which was the reason why ChCl/EG worked better than ChCl/CA for TPs extraction.

The interaction energies (E_{INT}) between HBA and HBD of the NADES, as well as those between the solute EGCG and different solvents were calculated. The result showed that the E_{INT} value between ChCl and CA was about -50.8057 kJ/mol, which was very strong, while that between ChCl and EG was about -35.9308 kJ/mol. These implied the stronger interaction between the HBA and HBD of ChCl/CA than ChCl/EG. By contrast, the E_{INT} value between ChCl/EG and EGCG was about -41.9727 kJ/mol, while that between ChCl/CA and EGCG was only about -19.9295 kJ/mol, which greatly supported the aforementioned inferences. These results were also complementary to the analysis of σ-profiles in Figs. 2, 4 and 5, as well as the $\gamma\infty$ in Fig. 3.

As for the two traditional solvents, water and ethanol, both were relatively weak in the HBA and HBD region, which can be used to explain the lower extraction yield of these traditional solvents. The difference of extraction yield with ethanol and water might attribute to the fact that ethanol had higher peaks in the non-polar region when compared with that of water.

In a word, the COSMO-SAC simulation could be explored as a useful tool for the prediction of the extraction performance of different solvents, as well as helping to understand the molecular interaction during the extraction process in our study.

3.3. Extraction process optimization of TPs with ChCl/EG

There are many factors that can influence extraction efficiency, thus it is important to optimize extraction procedure. Based on the result of the single factor experiment, the optimization was carried out with BBD of RSM. The extraction yield of TPs from BBD experiments is summarized as in Table 3.

Design Expert 8.0.6 was employed for further ANOVA analysis of the response and variances. The summary of the analysis is shown in Table 4. Among the test variables used in the study, the influence of C, BD, A^2, B^2, C^2 and D^2 on extraction yield was very significant ($p < 0.05$), while that from AC, BC was significant ($0.05 < p < 0.1$). Dai et al. and his coworkers [24] investigated the phenolic extraction from safflower with three NADESs, and the results showed that water content had the biggest effect. From our study, the influence of water content was insignificant. The discrepancy about the influence of water content can be attributed to the facts that different NADESs were employed, and the range of water content investigated was different. Moreover, the polarity of products differed a lot.

When looking at the ANOVA analysis, the F-value of 11.43 with p-value < 0.0001 indicated that the model fitness was significant. Values of "Prob > F" greater than 0.1000 indicate the model terms are not significant. The "Lack of Fit F-value" of 0.91 implies the "Lack of Fit" is not significant relative to the pure error. There is a 58.92% chance that a

Table 3
Extraction yield of TPs with Box-Behnken design.

Runs	A	B	C	D	Yield (%)
1	0	−1	0	−1	16.54
2	0	1	0	−1	18.27
3	−1	1	0	0	16.94
4	1	−1	0	0	16.66
5	0	−1	1	0	18.20
6	0	−1	−1	0	17.94
7	0	−1	0	1	18.49
8	1	0	0	1	16.00
9	1	1	0	0	17.02
10	1	0	−1	0	16.11
11	1	0	1	0	15.48
12	−1	0	−1	0	15.43
13	0	0	0	0	19.96
14	0	0	−1	1	15.89
15	0	0	0	0	20.13
16	0	0	−1	−1	16.69
17	−1	0	0	1	15.91
18	−1	−1	0	0	16.54
19	−1	0	0	−1	15.96
20	0	0	0	0	18.87
21	−1	0	1	0	17.34
22	0	1	1	0	18.64
23	0	1	−1	0	16.21
24	0	0	0	0	20.43
25	0	0	1	1	16.12
26	0	0	1	−1	18.29
27	0	0	0	0	20.35
28	0	1	0	1	17.48
29	1	0	0	-1	16.03

Table 4
ANOVA analysis of variance and model.

Source	Sum of squares	df	Mean square	*F* value	*p* (Prob>*F*)
Model	59.37	14	4.24	11.43	<0.0001
A-Time	0.066	1	0.066	0.18	0.6801
B-Temperature	0.00299	1	0.00299	0.00807	0.9297
C- Liquid to solid ratio	2.74	1	2.74	7.39	0.0166
D-Water content	0.30	1	0.30	0.81	0.3845
AB	0.00034	1	0.00034	0.00092	0.9763
AC	1.53	1	1.53	4.13	0.0616
AD	0.000075	1	0.000075	0.0002	0.9888
BC	1.17	1	1.17	3.15	0.0976
BD	1.89	1	1.89	5.08	0.0407
CD	0.46	1	0.46	1.25	0.2820
A^2	36.78	1	36.78	99.11	<0.0001
B^2	3.19	1	3.19	8.60	0.0109
C^2	14.94	1	14.94	40.26	<0.0001
D^2	16.79	1	16.79	45.26	<0.0001
Residual	5.20	14	0.37		
Lack of Fit	3.61	10	0.36	0.91	0.5892
Pure Error	1.58	4	0.40		
Core total	64.57	28			

"Lack of Fit *F*-value" this large could occur due to noise. Since we want the model to fit, this non-significant lack of fit is good. The "Predicted R-Squared" of 0.6393 is in reasonable agreement with the "Adjusted R-Squared" of 0.8391. The coefficient of variance (CV) was 3.51%, which was not greater than 10%, thus this model normally can be considered reproducible. The "Adeq Precision" measures the signal to noise ratio. A ratio greater than 4 is desirable. The ratio of 11.234 indicates an adequate signal. In a word, this model can be used to navigate the design space.

The 3-D surface and contour graphs illustrating the interactions of A (time), B (temperature), C (liquid to solid ratio) and D (water content) on the TPs extraction yield are drawn and shown as in supplementary material, Figs. S1 and S2. It was obvious that the contour graph of BD was a very obvious oval shape, followed by AC and BC, while these of CD, AB and AD were roughly circular (as shown in Fig. S2), which implied the interaction between B and D was significant ($p < 0.05$), but the interactions between C and D, A and B, A and D, were negligible. This was in agreement with the ANOVA analysis from Table 4.

The final mathematical equation expressing the relationship of TPs with variables for prediction of TPs extraction yield, is as following (in terms of coded factors),

$$\begin{aligned}\text{Yield}\ (\%) = {} & 19.95 - 0.074A + 0.016B \\ & + 0.48C - 0.16D - 0.0092AB - 0.62\,AC + 0.0043\,AD \\ & + 0.54BC - 0.69BD - 0.34CD - 2.38A^2 - 0.70B^2 - 1.52C^2 - 1.61D^2\end{aligned}$$

The optimal parameters for TPs extraction using ChCl/EG (molar ratio 1:2) were as following, liquid to solid ratio of 44, 84 °C for 39 min, with a water content of 29%. The highest extraction yield of about 20.01% could be obtained from the prediction of the model. Duplicated experiments for verification of TPs extraction were carried out under the optimal condition. The extraction yield was about 20.12%, which fitted well with the prediction.

4. Conclusion

We examined a range of NADESs which composed of ChCl with different HBDs to extract TPs from green tea. The use of the NADESs, especially ChCl/EG (molar ratio 1:2), can effectively increase extraction efficiency when comparing with the traditional solvents. Further optimization of TPs extraction with ChCl/EG by RSM generated a perfect regression prediction model, and with the optimal conditions, the highest TPs extraction yield of 20.12% could be achieved, highlighting the potential of NADES for TPs extraction.

Meanwhile, the extraction performance of the solvents was interpreted by the analysis of their σ-profiles, the activity coefficient at infinite dilution (γ^{∞}) and the interaction energy (E_{INT}). The higher calculated $\ln\gamma^{\infty}$ via COSMO was correlated with the lower extraction yield from the experiment. Based on computational results, the combination of ChCl, a strong HBA, with EG, a relatively weaker HBD, resulted in a NADES with a stronger affinity to TPs. The COSMO-SAC methodology appears to be a useful tool to determine the extractability of TPs in different solvents, indicating its promising prospect in screening effective solvent for bioactive components extraction in further research.

Declaration of Competing Interest

The authors declare that they have no known competing financial interests or personal relationships that could have appeared to influence the work reported in this paper.

Acknowledgements

This work was supported by the Key Laboratory of Bio-based Material, Qingdao Institute of Bioenergy and Bioprocess Technology, Chinese Academy of Sciences (No. KLBM2016003).

Appendix A. Supplementary data

Supplementary data to this article can be found online at https://doi.org/10.1016/j.molliq.2021.115406.

References

[1] A.R. Khalatbary, E. Khademi, Nutr. Neurosci. 23 (2020) 281.
[2] X.J. Wang, Y. Feng, C.F. Chen, H. Yang, X.P. Yang, LWT-Food Sci. Technol. 131 (2020) 109810.
[3] Y. Yang, T. Zhang, Molecules 24 (2019) 816.
[4] Y. Miyata, Y. Shida, T. Hakariya, H. Sakai, Molecules 24 (2019) 193.
[5] S.K. Connors, G. Chornokur, N.B. Kumar, Nutr. Cancer 64 (2012) 4.
[6] R.S. Bruno, J.A. Bomser, M.G. Ferruzzi, in: V. Preedy (Ed.), Processing and Impact on Antioxidants in Beverages, Academic Press, New York 2014, pp. 33–39.

[7] A. Kosińska, W. Andlauer, in: V. Preedy (Ed.), Processing and Impact on Antioxidants in Beverages, Academic Press, New York 2014, pp. 109–120.
[8] V.M. MartÍNez, I.D. AristizÁBal, E.L. Moreno, Rev. Vitae (2017) 47.
[9] K.B. Sankalpa, S.M. Mathew, Int. J. Agri. Environ. Biotechnol. 10 (2017) 209.
[10] P.V.S. Kumar, S. Basheer, R. Ravi, M.S. Thakur, J. Food Sci. Technol. 48 (2011) 440.
[11] J. Liao, B. Qu, D. Liu, N. Zheng, Ultrason. Sonochem. 27 (2015) 110.
[12] Y. Zhang, X. Xia, M. Duan, Y. Han, J. Liu, M. Luo, C. Zhao, Y. Zu, Y. Fu, J. Mol. Catal. B Enzym. 123 (2016) 35.
[13] E. Zurob, R. Cabezas, E. Villarroel, N. Rosas, G. Merlet, E. Quijada-Maldonado, J. Romero, A. Plaza, Sep. Purif. Technol. 248 (2020) 1.
[14] S. Chanioti, C. Tzia, LWT-Food Sci. Technol. 79 (2017) 178.
[15] W. Ma, K.H. Row, J. Liq. Chromatogr. R. T. 40 (2017) 459.
[16] W. Liu, K. Zhang, J. Chen, J. Yu, J. Mol. Liq. 260 (2018) 173.
[17] C. Florindo, L.C. Branco, I.M. Marrucho, Fluid Phase Equilib. 448 (2017) 135.
[18] F. Peng, P. Xu, B.-Y. Zhao, M.-H. Zong, W.-Y. Lou, J. Food Sci. Technol. 55 (2018) 2326.
[19] B.Y. Zhao, P. Xu, F.X. Yang, H. Wu, M.H. Zong, W.Y. Lou, ACS Sustain. Chem. Eng. 3 (2015) 2746.
[20] S. Bajkacz, J. Adamek, Talanta 168 (2017) 329.
[21] B. Zhuang, L.L. Dou, P. Li, E.H. Liu, J. Pharm. biomed. 134 (2017) 214.
[22] W. Bi, M. Tian, K.H. Row, J. Chromatogr. A 1285 (2013) 22.
[23] Z. Wei, X. Qi, T. Li, M. Luo, W. Wang, Y. Zu, Y. Fu, Sep. Purif. Technol. 149 (2015) 237.
[24] Y. Dai, G.J. Witkamp, R. Verpoorte, Y.H. Choi, Anal. Chem. 85 (2013) 6272.
[25] A. Klamt, J. Phys. Chem. 99 (1995) 2224.
[26] A. Klamt, Fluid Phase Equilib. 407 (2016) 152.
[27] J. Scheffczyk, C. Redepenning, C.M. Jens, B. Winter, K. Leonhard, W. Marquardt, A. Bardow, Chem. Eng. Res. Des. 115 (2016) 433.
[28] M.K. Hadj-Kali, S. Mulyono, H.F. Hizaddin, I. Wazeer, L. El-Blidi, E. Ali, M.A. Hashim, I.M. Alnashef, Ind. Eng. Chem. Res. 55 (2016) 8415.
[29] H.F. Hizaddin, A. Ramalingam, M.A. Hashim, M.K.O. Hadj-Kali, J. Chem. Eng. Data 59 (2014) 3470.
[30] N. Turkmen, F. Sari, Y.S. Velioglu, Food Chem. 99 (2006) 835.
[31] M. Diedenhofen, A. Klamt, Fluid Phase Equilib. 294 (2010) 31.
[32] K.A. Kurnia, F. Lima, A.F.M. Cláudio, J.A.P. Coutinho, M.G. Freire, Phys. Chem. Chem. Phys. 29 (2015) 18980.
[33] L.Z. Zhang, X.B. Bing, Z.Q. Cui, J.A. Labarta, D.M. Xu, J. Gao, S.X. Zhou, Y.L. Wang, ACS Sustain. Chem. Eng. 8 (2020) 5662.
[34] S.-T. Lin, S.I. Sandler, Ind. Eng. Chem. Res. 41 (2002) 899.
[35] C.-M. Hsieh, S.I. Sandler, S.-T. Lin, Fluid Phase Equilib. 297 (2010) 90.
[36] D.M. Xu, M. Zhang, J. Gao, L.Z. Zhang, S.X. Zhou, Y.L. Wang, Chem. Eng. Commun. 206 (2019) 1199.
[37] S.L. Ferreira, R.E. Bruns, H.S. Ferreira, G.D. Matos, J.M. David, G.C. Brandao, E.G. da Silva, L.A. Portugal, P.S. dos Reis, A.S. Souza, W.N. dos Santos, Anal. Chim. Acta 597 (2007) 179.
[38] J. Sangster, J. Phys. Chem. Ref. Data 18 (1989) 1111.
[39] PubChem, Open Chemistry Database at the National Institutes of Health (NIH), USA, https://pubchem.ncbi.nlm.nih.gov/ 2021 (accessed 10 January 2021).
[40] Y. Huang, F. Feng, J. Jiang, Y. Qiao, T. Wu, J. Voglmeir, Z.G. Chen, Food Chem. 221 (2017) 1400.
[41] X. Chang, S. Lin, G. Wang, C. Shang, Z. Wang, K. Liu, Y. Fang, P.J. Stang, J. Am. Chem. Soc. 142 (2020) 15950.
[42] M.M. Lubtow, M.S. Haider, M. Kirsch, S. Klisch, R. Luxenhofer, Biomacromolecules 20 (2019) 3041.
[43] A. Klamt, COSMO-RS:From Quantum Chemistry to Fluid Phase Thermodynamics and Drug Design, Elsevier, Amsterdam, The Netherlands, 2005.
[44] Y. Chen, S. Zhou, Y. Wang, L. Li, Fluid Phase Equilib. 451 (2017) 12.
[45] A. Klamt, Fluid Phase Equilib. 172 (2000) 43.
[46] C.B. Bavoh, B. Lal, O. Nashed, M.S. Khan, L.K. Keong, M.A. Bustam, Chin. J. Chem. Eng. 24 (2016) 1619.
[47] H. Mori, H. Kugisaki, Y. Inokuchi, Nobuyuki Nishi, E. Miyoshi, K. Sakota, K. Ohashi, H. Sekiya, J. Phys. Chem. A 106 (2002) 4886.
[48] H. Cheng, C. Liu, J. Zhang, L. Chen, B. Zhang, Z. Qi, Chem. Eng. Process. 125 (2018) 246.
[49] M. Wlazło, E.I. Alevizou, E.C. Voutsas, U. Domańska, Fluid Phase Equilib. 424 (2016) 16.
[50] T.C. Jelinski, J. Mol. Model. 24 (2018) 180.
[51] D. Lee, W. Go, J. Oh, J. Lee, I. Jo, K.-S. Kim, Y. Seo, Chem. Eng. J. 399 (2020).
[52] T. Aissaoui, Y. Benguerba, I.M. AlNashef, J. Mol. Struct. 1141 (2017) 451.
[53] H. Sun, Y. Li, X. Wu, G. Li, J. Mol. Model. 19 (2013) 2433.
[54] S. Mulyono, H.F. Hizaddin, I.M. Alnashef, M.A. Hashim, A.H. Fakeehaa, M.K. Hadj-Kali, RSC Adv. 4 (2014) 17597.
[55] L. Zhou, J. Xu, Limei Xu, X. Wu, J. Chem. Phys. 150 (2019) 24505.
[56] B. Ozturka, M. Gonzalez-Miquel, Sep. Purif. Technol. 227 (2019) 115707.
[57] G. Gonfa, M.A. Bustam, A.M. Sharif, N. Mohamad, S. Ullah, J. Nat. Gas Sci. Eng. 27 (2015) 1141.